International Journal of Architectural, Civil and Construction Sciences
ISSN: 2415-1734
Vol:12, No:11, 2018

Theoretical, Numerical and Experimental Assessment of Elastomeric Bearing Stability

Manuel A. Guzman, Davide Forcellini, Ricardo Moreno, Diego H. Giraldo

***Abstract*—**Elastomeric bearings (EB) are used in many applications, such as base isolation of bridges, seismic protection and vibration control of other structures and machinery. Their versatility is due to their particular behavior since they have different stiffness in the vertical and horizontal directions, allowing to sustain vertical loads and at the same time horizontal displacements. Therefore, vertical, horizontal and bending stiffnesses are important parameters to take into account in the design of EB. In order to acquire a proper design methodology of EB all three, theoretical, finite element analysis and experimental, approaches should be taken into account to assess stability due to different loading states, predict their behavior and consequently their effects on the dynamic response of structures, and understand complex behavior and properties of rubber-like materials respectively. In particular, the recent large-displacement theory on the stability of EB formulated by Forcellini and Kelly is validated with both numerical simulations using the finite element method, and experimental results set at the University of Antioquia in Medellin, Colombia. In this regard, this study reproduces the behavior of EB under compression loads and investigates the stability behavior with the three mentioned points of view.

***Keywords*—**Elastomeric bearings, experimental tests, numerical simulations, stability, large-displacement theory.

I. State of the Art

EB act as energy dissipators in bridges, buildings and power generation plants and serve as base isolation, seismic protection and vibration control of structures and machinery. Besides simplicity and low maintenance requirements compared to alternative isolation systems, they are characterized by their versatility since their vertical stiffness allows sustaining vertical loads and their horizontal stiffness allows horizontal displacements. In bridges, EB generally connects the girder and piers supporting large static loads due to the weight of the structure and dynamic loads due to vehicular traffic, wind, thermal expansion, and seismic activity [1], [2]. Therefore, vertical, horizontal, and bending stiffnesses are important parameters to take into account in the design of EB, and consequently their effects on the dynamic response of structures.

Initial insights regarding the design parameters of EB were performed by Roeder and Stanton [3], [4] for the National Cooperative Highway Research Program (NCHRP) in order to update the American specifications for the seismic isolation design of highway bridges [5]. Later, several analytical models that explain the behavior of EB were proposed [6]-[13]. Nowadays, with the advances in computational development, numerical simulations using finite element modeling (FEM) can provide a strong tool to designers, besides theoretical and experimental approaches, to improve their understanding on the behavior of EB. A literature review upon these three approaches is here summarized.

Studies on theoretical approaches and development of analytical models [6]-[13] have been performed in order to assess the behavior of EB. Among them, Koh and Kelly [6] developed a simple mechanical linear model based on the Haringx [14] theory of the stability of solid rubber rods, later applied by Gent [15] in 1964. Later, Nagarajaiah and Ferrell [7], and Vemuru et al. [9], [10] proposed analytical models that take into account nonlinear behavior. Other models, like Forcellini and Kelly [8] model, study the stability of EB subjected to large deformations. This theory is able to predict buckling in tension and compression, interaction between vertical load and horizontal stiffness, and between vertical stiffness and horizontal displacements. Han and Warn [11] proposed a different model from previous semi-empirical approaches. Thus, this model is based on parameters that are related only to the material and geometry. The macroscopic model proposed by Iizuka [12], and the three-dimensional analytical model of Kikuchi et al. [13] are models also based on stability and large deformations. In some cases, models were verified by performing experimental tests or with experimental data from other authors [7], [9], [10], [13].

Different studies using numerical simulations have been also performed [16]-[23]. Among them, Warn and Weisman [16] used a finite element (FE) model to predict critical loads of EB, showing that the critical load capacity reduces with lateral displacements. Kumar et al. [17] used several mathematical models coded in OpenSees in order to reproduce the performance of EB under compression and tension. Wang et al. [18] performed analytical simulations in LS-DYNA of bridge EB using a hyper-viscoelastic model for rubber and studied the interaction effects under compression, bending and torsion taking into account material and geometrical nonlinearities. In studies performed by Forcellini [19] and Forcellini et al. [20], the large deformation response theory [8] was analyzed performing numerical simulations using OpenSees and ABAQUS respectively. Kalfas and Mitouilis [21] used different fluctuating axial displacements, shear

M. A. Guzman, Ph.D. student at the University of Antioquia, Medellin, Antioquia, Calle 67 No. 53 – 108, Colombia (corresponding author, phone: (+57 4) 2195550; e-mail: malberto.guzman@udea.edu.co).

D. Forcellini is with the University of San Marino, Via Salita la Rocca, 44 San Marino. (e-mail: davide.forcellini@unirsm.sm).

R. Moreno and D. H. Giraldo, Professor at the Mechanical Engineering Department, University of Antioquia, Medellin, Antioquia, Calle 67 No. 53 – 108, Colombia (e-mail: ricardo.moreno@udea.edu.co, dhernan.giraldo@udea.edu.co).

strains and rotation to study the stress distribution within the elastomer and steel shims with numerical analyses using ABAQUS. Najjar et al. [22] also used ABAQUS to study the influence of the number of rubber layers, thickness of steel shims and shear modulus on the vertical stiffness. Yang et al. [23] analyzed the vertical stiffness degradation of circular, annular, square and rectangular bearings. And in the same way as theoretical approaches, few studies incorporate experimental validation [17]-[19].

Finally, other experimental studies of bearings under compression [24]-[28] have been conducted to assess mechanical properties and performance of EB. Among them, Mori et al. [24] performed compressive tests using small load cells in order to measure stress levels in the top and bottom faces of bearings, and calculated the compressive stiffness. Chou and Huang [25] investigated not only cyclic compression, but the effect of thermal aging on several dynamic properties such as stiffness, energy absorption and viscous damping coefficient of neoprene rubber bearings. These effects should be taken into account in the design process of seismic isolated structures. Manos et al. [26] investigated several properties such as stiffness and damping ratio under axial loading. In other study performed by Oh and Kim [27], the long-term creep deflection was calculated performing compression creep tests. Burtscher and Dorfmann [28] also performed compression tests to EB with an anisotropic design introducing steel reinforcing plates to form a given angle with respect to the horizontal plane.

In this work, analytical, numerical, and experimental approaches will be considered at the same time in order to assess the behavior of EB. Numerical simulations using the FE method and uniaxial compressive tests to an EB specimen were performed in order to validate the recent large-displacement theory on the stability of EB proposed by Forcellini and Kelly [8].

II. Case Study

A squared EB of 150 mm of side length with seven rubber layers (t = 4 mm in thickness of each layer including top and bottom covers), and 1 mm thick steel shims was manufactured using a carbon black-filled natural rubber compound with 55 Shore A hardness (the geometric layout in Fig. 1 shows the dimensions of the bearing). The shape factor S for a single rubber layer, defined as the ratio of the load area to the bulge area [29], is 8.75 and calculated according to (1).

$$S = \frac{(length)(width)}{2t(length + width)} \quad (1)$$

A. Experimental Test

Uniaxial compressive tests (Fig. 2) were performed in a SHIMADZU AGS series universal testing machine with a 350 kN load cell at room temperature, and a testing speed of 5 mm/min at the Material Resistance Laboratory at the University of Antioquia in Medellin, Colombia. Fig. 3 shows the force-displacement curve of the uniaxial compressive test. Moreover, uniaxial compressive and pure shear tests to standardized specimens of the rubber compound were performed using a SHIMADZU AGS series universal testing machine with a 50 kN load cell at room temperature following the recommendations of ASTM standards [30], [31]. Tests were performed at the Polymer Processing Laboratory at the University of Antioquia in Medellin, Colombia. Mean values of the compression and shear modulus are: 4.341 ± 0.265 MPa and 0.626 ± 0.032 MPa respectively.

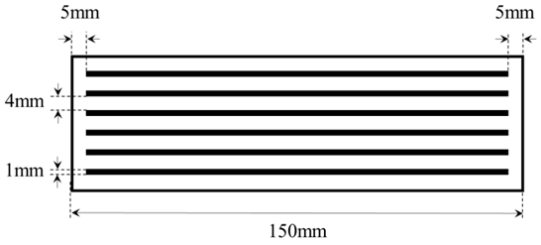

Fig. 1 Geometric layout of the EB tested

Fig. 2 Uniaxial compressive test

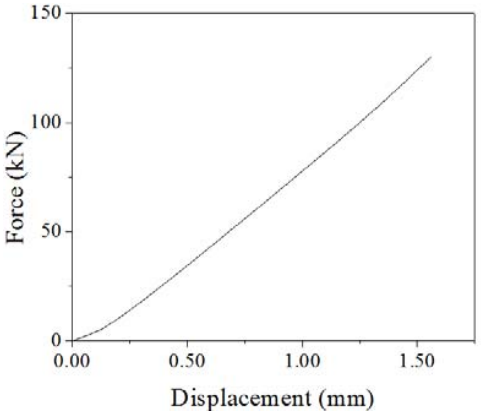

Fig. 3 Force-displacement curve of the uniaxial compressive test

B. Analytical Model

The theory derived by Forcellini and Kelly [8] predicts that the buckling load, taking into account large deformations, is given by the quadratic equation:

$$P^2 \frac{\cos\theta \sin\theta}{P_S} + P\sin\theta - P_E(\theta - \theta_0) = 0 \quad (2)$$

where P is the vertical load, $P_E = (\pi^2 EI_S)/h^2$ the Euler load

for a standard column (EI_S the bending stiffness), $P_S = GA_S = GAh/t_r$ the shear stiffness of a unit element of an isolator, and θ the relative rotation of the mechanical model used by [8] illustrated in Fig. 4. In addition, imperfections such as fabrication, geometric or material variations, are considered into an initial θ_0 angle.

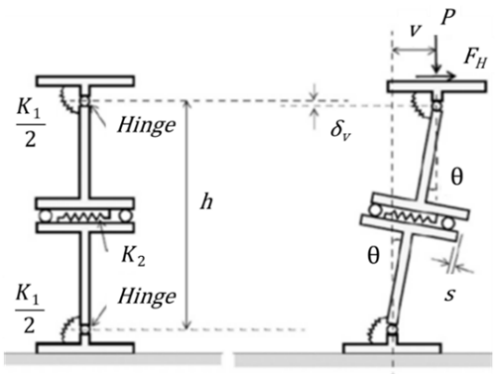

Fig. 4 Two-spring model used by Forcellini and Kelly [8]

The compressive stiffness is calculated as

$$E = \frac{F_c tn}{Ad_c} \tag{3}$$

where F_c is the compressive force from the experimental tests, t the thickness of a single rubber layer, n the number of rubber layers, A the loading area of the EB, d_c the experimental vertical displacement, and h the total height of the EB including internal steel shims. It is observed that the compressive modulus E is calculated on each step of the compressive test, leading to a variable modulus that is function of the force and of geometrical aspects of the EB. This variation of the compressive modulus is taken into account since this mechanical property depends on the shape factor [32].

From (2), the vertical load P can be calculated directly as

$$P = -\frac{P_S}{2\cos\theta} + \sqrt{\frac{P_S^2}{4\cos^2\theta} + \frac{P_E P_S(\theta - \theta_0)}{\sin\theta\cos\theta}} \tag{4}$$

Considering the large deformation kinematics in [8] and using the simple mechanical model shown in Fig. 3, the theoretical vertical displacement δ_v in terms of the shear displacement s is

$$\delta_v = s\sin\theta + (1-\cos\theta)h \tag{5}$$

and since

$$\frac{s}{h} = \frac{P}{P_S}\sin\theta + \frac{F_H}{P_S}\cos\theta \tag{6}$$

In the case of only vertical loading, the second term related to the horizontal force F_H is zero. Then the vertical displacement can be calculated as

$$\delta_v = \frac{P}{P_S} h\sin^2\theta + (1-\cos\theta)h \tag{7}$$

In order to apply the theory, it was necessary to calibrate θ_0. In this regard, a parametric study of θ_0 was performed. The values have been varied between 0.055 and 0.075 rad. Fig. 5 shows the different values of θ_0 plotted together. The black thick line represents the results obtained by the experimental compressive test.

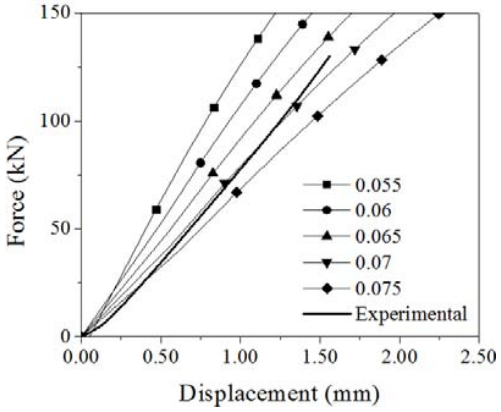

Fig. 5 Force-displacement curves for different values of θ_0

Fig. 6 shows the theoretical results obtained for the vertical load P, the relative rotation θ, and vertical displacement δ_v for a θ_0 value of 0.07. It is observed in Figs. 6 (a) and (b) that relative low values of the relative rotation θ (a maximum value of 0.1) were chosen since no horizontal displacements were applied. Moreover, large values of θ_0 can be attributed to imperfections as mentioned earlier and geometric variations which can include the relative low shape factor.

C. Numerical Simulations

In order to simulate the EB behavior, a FEM was built using OpenSees [33] (Open System for Earthquake Engineering Simulations) developed by Pacific Earthquake Engineering Center, which allows high level of advanced capabilities in modeling nonlinear responses using a wide range of material models, elements and solution algorithms. Numerical simulations are performed in the interface OpenSeesPL [34] which is originally calibrated for soil analyzes. In this study, the software is used to reproduce EBs since it is able to reproduce layered systems (alternating rubber and steel layers) and simulate realistic lateral boundaries built up by assuming shear beam conditions [19] which are typical conditions observed in EB performance.

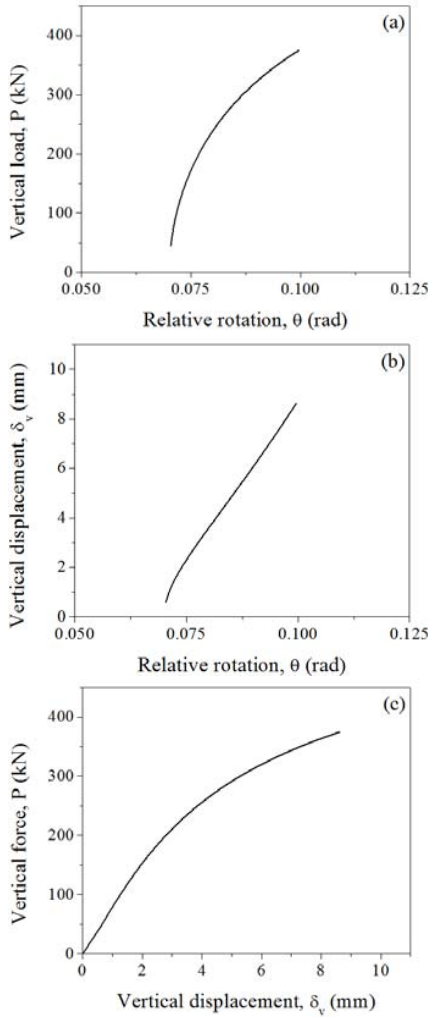

Fig. 6 Theoretical results of the vertical load, vertical displacement, and relative rotation

To validate the numerical model, several parameters, namely the mesh and properties of the materials were taken into account to perform the numerical simulations assuming linear behavior. The 3D mesh has dimensions of 0.140 m x 0.140 m x 0.054 m (including top and bottom steel plates of 0.01 mm each), composed of 8-node brick elements. The nodes at the top and bottom plates were tied together representing rigid surfaces that simulate the rigid supports of the testing machine in contact with the EB. A mesh used in this study is shown in Fig. 7.

To simulate the uniaxial compressive test, a pushover analysis was performed using the forced-based method, within 10 steps with increments of 15 kN to reach a total of 150 kN. The backbone curves for both the rubber and the steel layers were considered linear and are respectively shown in Figs. 8 (a) and (b).

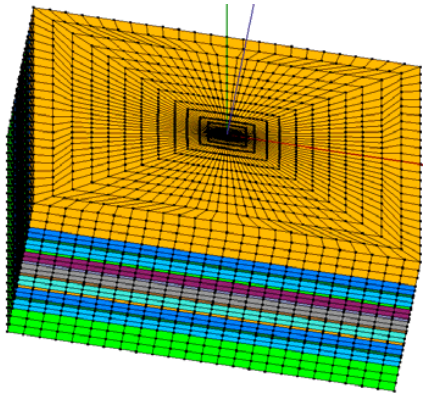

Fig. 7 Three-dimensional FEM built in OpenSeesPL

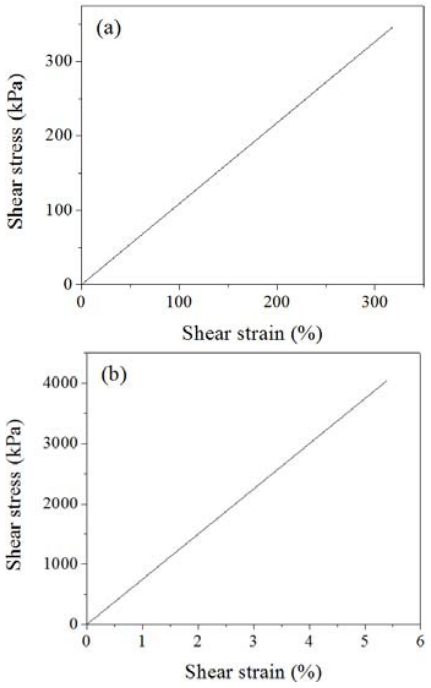

Fig. 8 Linear backbone curves for (a) rubber and (b) steel

Since OpenSeesPL is originally calibrated for soil analyzes, the accuracy of the numerical model was evaluated through several aspects of the model. Firstly, a convergence study of the mesh was performed. Fig. 9 shows the maximum vertical displacement of the different layers of the EB according to its elevation for different types of mesh. Meshes differ on the number of slices used in the analysis, thus the number of elements and nodes are tabulated in Table I.

It is observed in Fig. 9 that the meshes used in this analysis yield lower values of the vertical displacement, not larger than 0.0008 mm, compared to those obtained in the experimental tests. Therefore, numerical simulations of only layers of steel and rubber separately were performed to differentiate the behavior of each material using their linear properties according to the backbone curves shown in Fig. 8. The maximum vertical displacement of the layers of steel and

rubber accordingly to their elevation are presented in Fig. 10. As expected, due to the push over analysis, the vertical displacement of all rubber layers is greater that for the steel, because of the different stiffnesses used.

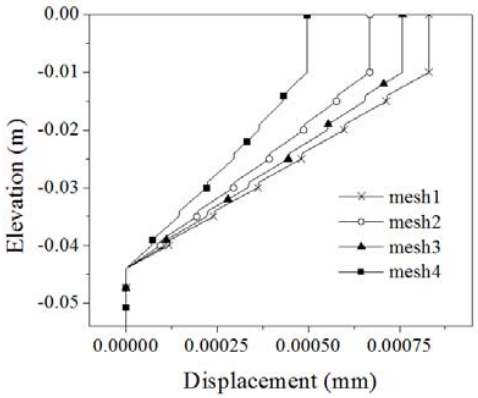

Fig. 9 Maximum vertical displacements for different meshes

TABLE I
MESH CHARACTERISTICS

Mesh	Number of elements	Number of nodes
1	31096	33723
2	33488	36315
3	35880	38907
4	39312	42363

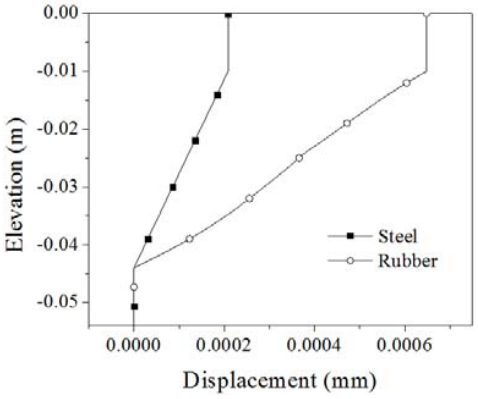

Fig. 10 Maximum vertical displacement assuming all layers of steel and rubber

III. Results and Discussion

Fig. 11 shows the theoretical and experimental results. It is observed that the large displacement theory proposed by Forcellini and Kelly [8] and experimental data agree even if the shape factor is relatively small (S = 8.75), if compared with typical shape factors that range from 10 to 30, and this could be an important aspect that defines large values of θ_0. It should be mentioned also that the tests were performed for relatively low displacements and only in compression, therefore the selection of low values of the relative rotation θ should be considered. Furthermore, postbuckling behavior was not studied since no horizontal displacements were taken into account. A significant aspect of the theoretical verification is the consideration of the compressive modulus as a variable mechanical property due to large geometric changes during the compressive loading, enhancing theoretical results.

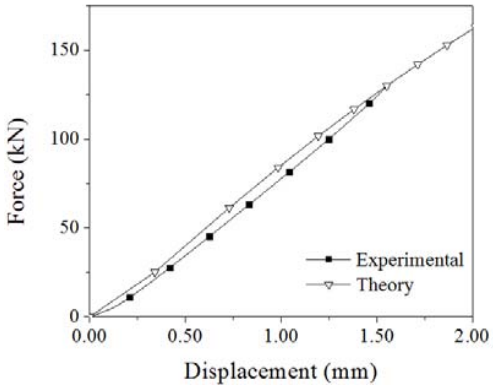

Fig. 11 Theoretical and experimental results

Numerical simulations using OpenSees (under hypothesis of linear materials), exhibit a response that is different to that resulted by the experimental and theoretical approaches. This can be due to the assumed linear behavior that is not adequate for numerical simulations. More analyses that can take into account nonlinear behavior of the materials will be object of further work.

IV. Conclusion

In this work, the large-displacement theory proposed by Forcellini and Kelly [8] was validated through uniaxial compressive tests and a study of numerical simulations using a FEM model built with OpenSeesPL. The theory is able to reproduce EB behavior in compression. In this regard, in order to validate the theory more accurately, the proper choice of the compressive modulus is fundamental, and it should be taken as a changing variable dependent to the deformation that takes place. In addition, the performed numerical simulations have a different force-displacement behavior compared to the results obtained experimental and theoretically. In this regard, more efforts should be made to model the material with nonlinear materials.

References

[1] O. Hamzeh, J. L. Tassoulas, and E. B. Becker, “Analysis of Elastomeric Bridge Bearings,” 1995.
[2] B. A. English, R. E. Klingner, and J. A. Yura, “Elastomeric Bearings: Background information and field study,” 1993.
[3] J. F. Stanton and C. W. Roeder, “NCHRP Report 248 - Elastomeric bearings design, construction, and materials,” 1982.
[4] C. W. Roeder, J. F. Stanton, and A. W. Taylor, “NCHRP Report 298 - Performance of elastomeric bearings,” 1987.
[5] American Association of State Highway and Transportation Officials, “AASHTO LRFD Bridge Design Specifications,” 2012.
[6] C. G. Koh and J. M. Kelly, “A simple mechanical model for elastomeric bearings used in base isolation,” Int. J. Mech. Sci., vol. 30, no. 12, pp. 933–943, 1988.
[7] S. Nagarajaiah and K. Ferrell, “Stability of Elastomeric Seismic Isolation Bearings,” J. Struct. Eng., vol. 125, pp. 946–954, 1999.
[8] D. Forcellini and J. M. Kelly, “Analysis of the large deformation

stability of elastomeric bearings," J. Eng. Mech., vol. 140, no. 6, pp. 1–10, 2014.
[9] S. M. V. Vemuru, S. Nagarajaiah, A. Masroor, and G. Mosqueda, "Dynamic Lateral Stability of Elastomeric Seismic Isolation Bearings," J. Struct. Eng., pp. 1–14, 2014.
[10] V. S. M. Vemuru, S. Nagarajaiah, and G. Mosqueda, "Coupled horizontal–vertical stability of bearings under dynamic loading," Earthq. Eng. Struct. Dyn., vol. 45, pp. 913–934, 2015.
[11] X. Han and G. P. Warn, "Mechanistic model for simulating critical behavior in elastomeric bearings," J. Struct. Eng., vol. 141, no. 5, p. 4014140, 2015.
[12] M. Iizuka, "A macroscopic model for predicting large-deformation behaviors of laminated rubber bearings," Eng. Struct., vol. 22, no. 4, pp. 323–334, 2000.
[13] M. Kikuchi, T. Nakamura, and I. D. Aiken, "Three-dimensional analysis for square seismic isolation bearings under large shear deformations and high axial loads Masaru," Earthq. Eng. Struct. Dyn., vol. 39, pp. 1513–1531, 2010.
[14] J. A. Haringx, "On highly compressible helical springs and rubber rods and their application for vibration-free mountings," Phillips Res. Reports, vol. Rep. 3, pp. 401–449, 1949.
[15] A. N. Gent, "Elastic stability of rubber compression springs," J. Mech. Eng. Sci., vol. 6, no. 4, pp. 415–430, 1964.
[16] G. P. Warn and J. Weisman, "Parametric finite element investigation of the critical load capacity of elastomeric strip bearings," Eng. Struct., vol. 33, no. 12, pp. 3509–3515, 2011.
[17] M. Kumar, A. S. Whittaker, and M. C. Constantinou, "Mechanical Properties of Elastomeric Seismic Isolation Bearings for Analysis Under Extreme loading," in 22nd Conference on Structural Mechanics in Reactor Technology, 2013.
[18] R. Z. Wang, S. K. Chen, K. Y. Liu, C. Y. Wang, K. C. Chang, and S. H. Chen, "Analytical Simulations of the Steel-Laminated Elastomeric Bridge Bearing," J. Mech., vol. 30, no. 4, pp. 373–382, 2015.
[19] D. Forcellini, "3D Numerical simulations of elastomeric bearings for bridges," Innov. Infrastruct. Solut., vol. 1, no. 1, p. 45, 2016.
[20] D. Forcellini, S. Mitoulis, and K. N. Kalfas, "Study on the response of elastomeric bearings with 3D numerical simulations and experimental validation," in 6th ECCOMAS Thematic Conference on Computational Methods in Structural Dynamics and Earthquake Engineering, 2017, p. 9.
[21] K. N. Kalfas and S. A. Mitoulis, "Performance of steel-laminated rubber bearings subjected to combinations of axial loads and shear strains," Procedia Eng., vol. 199, pp. 2979–2984, 2017.
[22] D. Najjar, A. Kaadan, M. N. A. Eilouch, and A. Al Helwani, "Multi-criteria decision making to improve the performance of base isolation rubber bearing," Asian J. Civ. Eng., vol. 18, no. 7, pp. 1095–1112, 2017.
[23] W. Yang, X. Sun, M. Wang, and P. Liu, "Vertical stiffness degradation of laminated rubber bearings under lateral deformation," Constr. Build. Mater. vol. 152, pp. 310–318, 2017.
[24] A. Mori, A. J. Carr, N. Cooke, and P. J. Moss, "Compression behaviour of bridge bearings used for seismic isolation," Eng. Struct., vol. 18, no. 5, pp. 351–362, 1996.
[25] H.-W. Chou and J.-S. Huang, "Effects of Cyclic Compression and Thermal Aging on Dynamic Properties of Neoprene Rubber Bearings," J. Appl. Polym. Sci., vol. 107, pp. 1635–1641, 2007.
[26] G. C. Manos, S. Mitoulis, V. Kourtidis, A. Sextos, and I. Tegos, "Study of the behavior of Steel Laminated Rubber Bearings under prescribed loads," in 10th World Conference on Seismic Isolation, Energy Dissipation and Active Vibrations Control of Structures, 2007, vol. 2, p. 12.
[27] J. Oh and J. H. Kim, "Prediction of long-term creep deflection of seismic isolation bearings," J. Vibroengineering, vol. 19, no. 1, pp. 355–363, 2017.
[28] S. L. Burtscher and A. Dorfmann, "Compression and shear tests of anisotropic high damping rubber bearings," Eng. Struct., vol. 26, no. 13, pp. 1979–1991, 2004.
[29] P. M. Sheridan, F. O. James, and T. S. Miller, "Design of Components," in Engineering with Rubber - How to Design Rubber Components, Third Edit., A. N. Gent, Ed. Carl Hanser Verlag GmbH & Co. KG, 2012, pp. 259–293.
[30] ASTM, D575-91: Standard Test Methods for Rubber Properties in Compression. 2012, pp. 1–4.
[31] ASTM, D945-06: Standard Test Methods for Rubber Properties in Compression or Shear (Mechanical Oscillograph). 2012, pp. 1–11.
[32] D. O. Fediuc, M. Budescu, V. Fediuc, and V.-M. Venghiac, "Compression Modulus of Elastomers," Bull. Polytech. Inst. Jassy, vol. 62, pp. 157–166, 2013.
[33] S. Mazzoni, F. McKenna, M. H. Scott, and G. L. Fenves, "OpenSees, Open System for Earthquake Engineering Simulation." University of Berkley, 2011.
[34] J. Lu, A. Elgamal, and Z. Yang, "OpenSeesPL - 3D Lateral Pile-Ground Interaction." 2012.